Fuel 154 (2015) 275–292

Contents lists available at ScienceDirect

Fuel

journal homepage: www.elsevier.com/locate/fuel

An extended mean value model (EMVM) for control-oriented modeling of diesel engines transient performance and emissions

Kamyar Nikzadfar *, Amir H. Shamekhi

Mechanical Engineering, K.N. Toosi University of Technology, Tehran, Iran

HIGHLIGHTS

- EMVM method for control-oriented modeling of diesel engine emissions is introduced.
- The block oriented modeling approach has been used for modeling the engine.
- The whole engine is assumed to be composed of distinct dynamic and static modules.
- The ANN is applied into MVM for prediction of emissions and performance.
- The developed model is validated using step and frequency response tests.

GRAPHICAL ABSTRACT

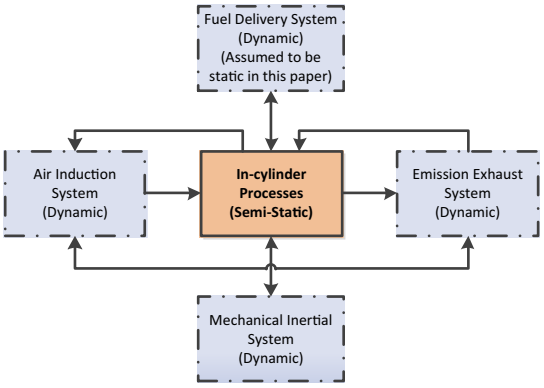

ARTICLE INFO

Article history:
Received 25 June 2014
Received in revised form 23 December 2014
Accepted 26 March 2015
Available online 7 April 2015

Keywords:
Extended mean value model
Control oriented engine model
Model-based controller design
Engine management systems
Diesel engine emission modeling

ABSTRACT

Utilizing model-based controller design in automotive and powertrain industry is recently attracting more attention due to its benefits in reducing controller development time and cost. Recent automotive emission legislations put more limits on engine emissions in transients. Hence, the models, which are capable of predicting engine performance and emissions in transient, are of the utmost importance. On the other hand, the model-based controller design requires accurate meanwhile fast to run models to be employed in both controller development and subsequent hardware in loop processes. In this paper, a new quasi-static control oriented diesel engine modeling approach is investigated based on the block oriented modeling method to predict the engine behavior in sense of both performance and emissions in transient and steady state operation. The accuracy and speed of model execution are two important attributes of models, which are in mutuality. In the proposed modeling a tradeoff between these two factors are made and some solutions are employed to increase both model accuracy and speed. The diesel engines are nonlinear dynamic systems. In the proposed modeling approach, this behavior is assumed to be composed of a semi-static combustion process surrounded by peripheral dynamic processes. This static in cylinder process model is responsible for the performance and emissions of the engine. Thermodynamic modeling coupled with chemical reaction model altogether with 1D gas dynamic model is employed to predict the performance and emission of in-cylinder process based on some boundary conditions which are derived from peripheral systems. Usually an iterative time consuming method is employed to solve the thermodynamic models. In order to decrease the run-time of model, a neural

Abbreviations: ANFIS, Adaptive Network Fuzzy Inference System; ANN, Artificial Neural Networks; BOM, Block Oriented Models; CR, Common Rail; DEM, discrete event model; EGR, Exhaust Gas Recirculation; EIS, Engine Inertial System; HiL, Hardware in Loop; ICP, In-Cylinder Process; IES, Intake and Exhaust System; LOLIMOT, Local Linear Model Tree; MVM, Mean Value Model; NARMAX, Nonlinear Auto-Regressive Moving Average with eXogenous inputs; SiL, Software in Loop; TC, Turbocharger; VGT, Variable Geometry Turbine; MIMO, multi input multi output; EMVM, extended mean value model.

* Corresponding author.
E-mail addresses: nikzadfar@dena.kntu.ac.ir (K. Nikzadfar), shamekhi@kntu.ac.ir (A.H. Shamekhi).

http://dx.doi.org/10.1016/j.fuel.2015.03.070

network is trained to mimic the thermodynamic model. On the other hand ordinary time differential equations are used to model the peripheral dynamic systems such as induction and exhaust systems. In order to validate the model for both steady and transient regimes, real step responses as well as experimental frequency response are compared with model results. The comparison of experimental data with model results shows tight agreement in both performance and emission prediction capabilities.

1. Introduction

Diesel engines are attracting more attention due to their inherent high efficiency and the potential to reduce their emissions. Nevertheless, the automotive manufacturers always face with stricter emission obligations, which force them to decrease the emission level of their products. On the other hand the customers require for more fuel economy. The performance, emissions and noise level of diesel engines strongly depend on the combustion phenomena, which can be effectively controlled by precise fuel injection and tuning the inducted air path parameters. Advent of the microcontrollers altogether with development of advanced control theories, paved the way of achieving clean and calm diesel engines.

Anyway, design and calibration of new control schemes is complex and time consuming and usually requires large amount of expensive tests. These all lead to advent of model-based control design procedure. The model-based control system development can significantly decrease the cost and time of control systems development, which is favorable to automotive manufacturers [1,2]. In model-based controller design procedure, precise meanwhile computationally efficient models are needed to simulate the engine behavior in transient modes. The developed model will not only be employed as a plant in controller design procedure, but also is used in Hardware in Loop (HiL), Software in Loop (SiL), fault diagnosis, hybrid electrical power train design, automatic transmission control, model-based calibration and engine-vehicle coincidence procedure. In the recent vehicle emission obligations, the role of transient engine operation has been highlighted, which in turn increased the need to a control-oriented model with emission prediction capabilities in transient operation. Due to the cost of emission sensors, they are not used in diesel engine control systems, such models can be employed in development of emission observers and estimators. Usually mean value models (MVM) are used for controller design aims. These models are usually inefficient to predict the engine emission in transient regime. On the other hand, the models, which are able to predict the emissions, are computationally complex and consequently not suitable for control purposes.

As complicated systems with a variety of sub systems, diesel engines are being considered from different points of view, each of them results into a class of modeling. Diesel engines behavior can be assumed to be originated from an air induction/exhaust gas dynamics system and a relatively fast combustion process. The dynamic behavior of engines is mainly due to gas flow systems while combustion process is directly responsible for emission and performance of engine. Due to this fact, two main modeling approaches are emerged in literatures: combustion modeling, which takes into account the thermodynamic aspects of combustion phenomena, and the dynamic modeling that considers the behavior of induction and exhaust systems. Thermodynamic models are mainly employed for prediction of emissions and performance of engines. Static combustion models can be categorized into three distinct categories: phenomenological approach which includes the governing physical models [3–5], empirical approach (black-box model) which includes the input–output data with an identification method [6,7] and a hybrid modeling (gray-box model) which are combination of the two mentioned approaches. On the other hand, dynamic models of engines are usually employed for control purposes [8]. The dynamic models can also be categorized to phenomenological based models which use governing physical equations to describe the systems dynamics [9] and empirical models which are developed based on identification of engine input–output time series data. The latter contains both classical approach like Nonlinear Auto-Regressive Moving Average with exogenous inputs (NARMAX) [10] and subspace method, [11] as well as modern soft computing approaches such as fuzzy [12], Adaptive Network Fuzzy Inference System (ANFIS) [13], Local Linear Model Tree (LOLIMOT) [14] and dynamic ANN [15]. Experimental data in time series format is employed to identify the models, which in turn increase dependency to costly and time consuming tests. The phenomenological dynamic models however consider the inlet and exhaust systems and the other modules, which cause the dynamic behavior of engine. MVM is the state of art modeling approach for engine dynamic behavior modeling [16]. It neglects the discrete cycles of engine and assumes all processes and effects that are spread out over the engine cycle. The combustion data is usually being taken into account by look-up tables or interpolated algebraic equation [9]. However, some efforts have been done to implement the crank angle based models directly into real time MVM models to predict the engine performance [17,18]. The tabulated method is rapid enough to be used for high-level controller development purpose but they have rarely been considered for modeling the emissions. Nevertheless, some efforts to implement emissions models as tabulated look-up tables or algebraic polynomial expression (based on engine speed and load) into MVM models can be found in literature [19,20,16,21]. Application of test bench steady state data into MVM leads to inefficient models, which cannot predict the emissions with desired accuracy in transient modes; usually correction factors are used to compensate for transient prediction errors [19,22]. The correction factors takes into account the dynamic effects of diesel engines such as turbo lag and gas dynamic delays. In addition, the thermodynamic modeling coupled with chemical reaction models has been implemented in MVM models. Unfortunately, this type of modeling is computationally inconsistent with real time applications and makes the model too slow to run for control purposes [4].

Anyway, development of modern diesel engine control systems requires the transient models which take into account the transient emission prediction and engine performance indices with low computational burden and required accuracy. As described earlier, the capabilities of emission prediction have been implemented in existing models in two way: directly embedding a thermodynamic-chemical reaction model into MVM model and using a RPM-Load tabulated emission map with compensating correction factors. The former leads to accurate but slow-to-run models, which are not suitable for control development and real-time requirement and the later is computationally favorable but lacks the required accuracy for model-based controller development and calibration aims.

In this paper, a new approach for control-oriented modeling of diesel engines is proposed with inspiration of Block Oriented Models (BOM), which can predict engine emissions in transients

Nomenclature

A_r	opening area of EGR valve
C	isentropic nozzle flow
c_p	specific heat in constant pressure
D	diameter of compressor blade
I_{en}	engine rotational inertia
I_{tc}	TC blades and interconnecting shaft rotational inertia
M	mach number
$\dot{m}_{as}$	engine aspirated mass flow rate
$m_{a,e}$	mass of air in exhaust manifold
$\dot{m}_c$	compressor mass flow rate
$\dot{m}_{c,cor}$	corrected compressor mass flow rate
m_e	accumulated whole accumulated mass of gas in exhaust manifold
$\dot{m}_{ex,a}$	mass flow rate of fresh air to exhaust manifold
$\dot{m}_{egr}$	the mass flow rate of EGR gas
m_f	the mass of injected fuel per cylinder in each cycle
m_i	accumulated whole accumulated mass of gas in inlet manifold
$\dot{m}_t$	turbine mass flow rate
$\dot{m}_{th}$	throttle valve mass flow rate
$m_{x,i}$	mass of burned gas in inlet manifold
P_a	ambient pressure
P_e	exhaust manifold pressure
P_i	inlet manifold air pressure
P_p	the pressure of air in compressor–throttle valve connecting pipe
$p_{r,egr}$	pressure ratio across the EGR valve
$p_{r,t}$	pressure ratio across the turbine
$p_{r,th}$	pressure ratio across the throttle valve
PW_c	compressor consumed power
PW_t	turbine generated power
T_a	ambient temperature
T_c	temperature of air after compressor
T_{cool}	coolant fluid temperature
T_e	exhaust manifold temperature
T_{egr}	temperature of EGR gas after intercooler
T_{ex}	temperature of engine exhaust gas
T_i	inlet manifold air temperature
T_{ic}	temperature of air after main intercooler
T_p	temperature of air in compressor–throttle valve connecting pipe
U	blade tip speed
V	flow velocity
V_e	exhaust manifold volume
V_i	inlet manifold volume
X_e	the ratio of burned gas to whole accumulated mass in exhaust manifold
x_{egr}	EGR valve opening signal
X_i	the ratio of burned gas to whole accumulated mass in inlet manifold
x_{th}	throttle valve opening percentage
x_{vgt}	the VGT opening signal

Greek letters

η_c	compressor thermodynamic efficiency
$\eta_{ic,c}$	compressor heat exchanger efficiency
$\eta_{ic,egr}$	EGR heat exchanger efficiency
η_t	turbine thermodynamic efficiency
ω_{eng}	engine rotational speed
$\omega_{tc,cor}$	corrected turbocharger speed
ψ	isentropic work coefficient (TC modeling)
γ	specific heat ratio
θ_{th}	throttle valve angle
ϕ	flow coefficient (TC modeling)
τ_b	generated engine net torque
τ_l	external load torque

with very low computational burden and required accuracy. BOM assumes that a nonlinear process is mainly composed of a linear dynamic systems followed by a nonlinear static system [23]. The whole engine system is divided to some subsystems; one of which is in-cylinder (combustion) system. The combustion process as the main source of engine emission and performance has been modeled using a detailed thermodynamic model coupled with involved chemical reaction. Since this kind of modeling is computationally inefficient, an artificial neural network (ANN) is employed to mimic the thermodynamic model results. A special care is dedicated to selecting the input and outputs so that no need to correcting factors exists. The whole model shows good properties in both run-time and accuracy aspects.

This paper begins with a brief description of test bench accessories. After which a brief description and supports for the proposed engine modeling approach is mentioned. The model architecture is described then and respective sub-models are developed in respective sections. Finally, the results are compared with experimental data to show the effectiveness of proposed modeling approach.

2. Experimental setup

In order to develop the model and identification of the unknown parameters and also validation of developed model a test setup has been developed. An AVL Dynoperform160 dynamometer is employed for applying the desired load both in steady state and transient mode. AVL PUMA open test and control system is employed as the main control system, it is also used for synchronization of other measuring devices and saving the test data. An air control unit is used for providing the engine with standard air. In order to measure the fuel flow, AVL Fuelexact system is used which offers no more than 0.1% error. Two distinct emission measuring units are used for measuring NOx and soot in transient mode. Horiba MEXA7100DEGR is employed for measuring generated NOX with 1% measurement error, while AVL Micro Soot Sensor is used for measuring generated soot. Also the MEXA7100DEGR is able to measure exhaust gas AFR and EGR rate. In order to validate the thermodynamic model, an in-cylinder pressure signal has been compared with model results. Pressure sensor GH13G is used for measuring the in-cylinder pressure while AVL Indismart module is employed for signal conditioning. The engine coolant control system is also used. An optical AVL TS350 sensor is used to measure the turbocharger speed. The pressure and temperature of required points are measured using appropriate sensors. The schematics of test setup are depicted in Fig. 1.

3. Engine modeling

In order to design the advanced electronic controllers for diesel engines, accurate models are needed which are able to model both performance and emissions. In this part, the concept of Extended MVM (EMVM) is described and will be employed to model the performance and raw emissions of a 1.5L Common Rail (CR) turbocharged diesel engine. The proposed method takes into account

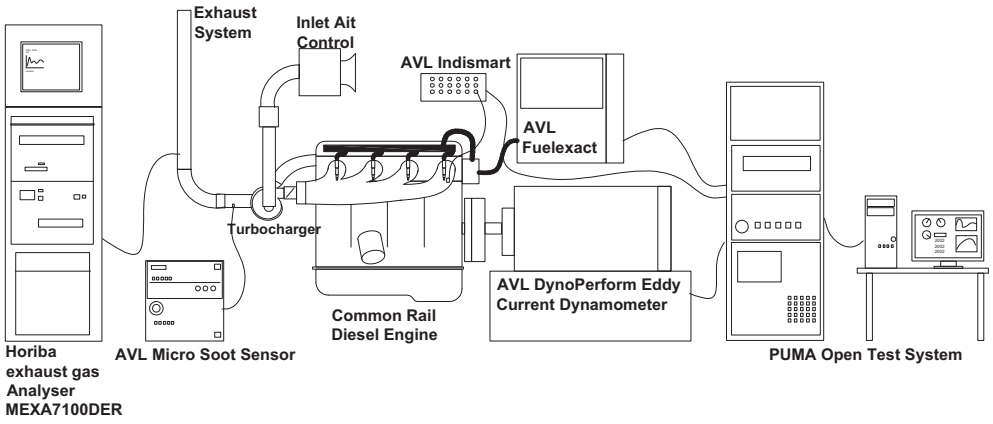

Fig. 1. The schematics of test setup.

the detailed thermodynamic aspects of engine while avoids high computational burden by utilizing Artificial Neural Networks (ANN). For detailed modeling, different parts of engine are modeled using phenomenological methods. The components of engine are depicted in Fig. 2; also different parts are numbered for modeling purposes. The engine comprises inlet/exhaust systems which are coupled together by a Variable Geometry Turbine (VGT) and Exhaust Gas Recirculation (EGR) path. Two intercoolers are employed for cooling the compressed air and EGR gas. The inlet air path possesses a throttle valve which is used when fast air pressure decrease is needed i.e. difference in manifolds pressures are not sufficient to drive desired exhaust gas flow into inlet manifold.

3.1. Modeling aims

By developing the microcontroller based diesel engine controller, more potential to decrease the engine emission are emerged. Design and calibration of diesel engine controllers which consider emission legislatives, requires models that are able to model both performance and emissions with desired level of accuracy. Developing the diesel engine control oriented models with ability of raw emissions prediction has received little attention [16]. In this paper, a new modeling method is developed based on existing MVM method with raw emission prediction capabilities. The model should be fast enough to be used in controller design procedure as well as HiL real time applications. Using new technologies in diesel engines increase the number of actuators which in turn increase the number of inputs to model. The model should be able to model the influence of different inputs on engine outputs (performance, emission and EMS sensor signals) in a time depended manner.

3.2. Modeling assumptions

Turbocharged diesel engines are complex nonlinear dynamic systems which are composed of coupled dynamic subsystems. BOM is a method to model the nonlinear dynamic systems. In this method, the whole system is assumed to be composed of a memory-less nonlinear system in series with a linear dynamic system [23]. In BOM the nonlinear behavior of system is completely assigned to a static system the dynamic behavior of the system is described by linear dynamic systems. This method of system

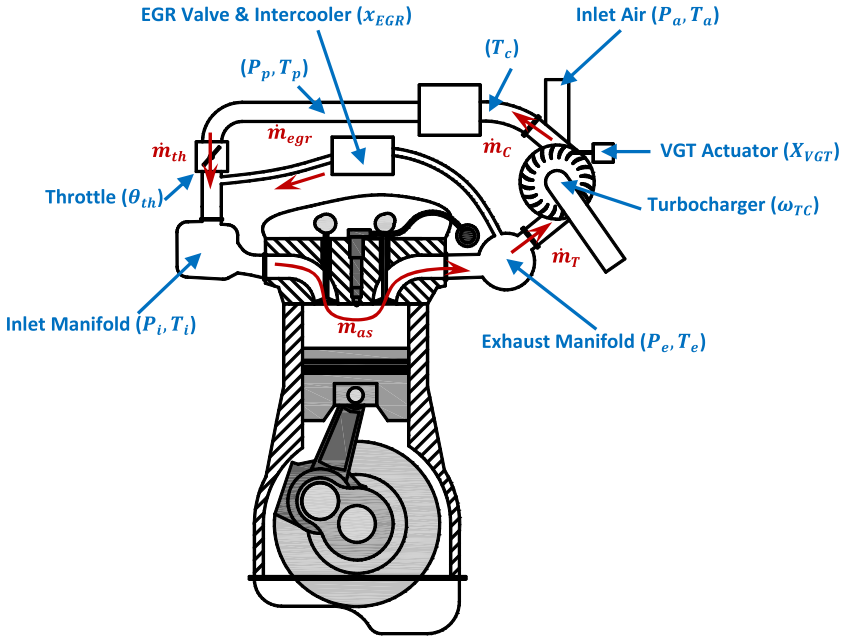

Fig. 2. The components of proposed turbocharged diesel engine [2].

behavior description inspired us to describe the engine behavior by dividing it to a static part and a dynamic part. The heart of diesel engine is a thermodynamic process which occurs in a closed cycle in one or two revolution of engine crank shaft. This fast process determines the engine emission and performance. In the MVM, the average of variables in 5–10 respective cycles is considered instead the cyclic or angle-based value of variables. These variables are memory-less nonlinear function of cylinder boundary conditions such as inlet air properties, fuel injection pattern and other engine operational parameters. Due to relatively fast cyclic process, the in-cylinder process (include combustion) can be assumed to be a semi-static process in comparison to other processes occur in diesel engines which are mainly responsible for providing air and fuel for cylinder. In the other words, combustion can be assumed a nonlinear memory-less procedure while its inputs are obtained by dynamic systems as depicted in Fig. 3. Fuel Delivery System (FDS) is a fast dynamic system when compared to other dynamic modules in system. Usually feedback controllers are used to control rail pressure in such manner that can vary rail pressure from 230 bar up to 1600 bar within a tolerance of 1% and steep gradients (e.g. up to 3000 bar/s) [24]. The fast dynamics of controlled systems let us ignore the dynamics of FDS in comparison to the other engine modules, so the dynamic FDS is modeled as a semi-static system in this paper.

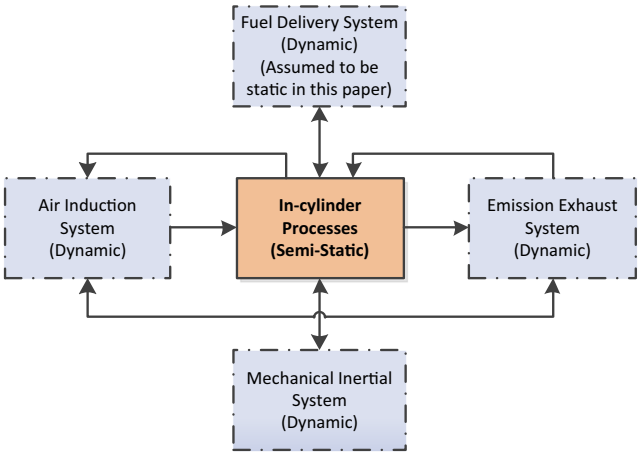

Fig. 3. The semi-static and dynamic engine sub-systems (Exogenous inputs not shown) [2].

The following assumptions are taken into account for modeling the sub-systems. Air induction and exhaust gas systems are two major dynamic systems to be modeled. Both fresh air and exhaust gases are assumed to be ideal gases. The lumped model is used for modeling the plenum air dynamics and the wave properties of air flow are neglected. The wall heat transfer and flow friction in pipes are neglected while port heat transfer is considered. Willans line is employed for modeling the mechanical friction based on test data.

3.3. Model architecture

The architecture of model is developed based on three main modules: Intake and Exhaust System (IES), In-Cylinder Process (ICP) and Engine Inertial System (EIS). The fuel delivery system is neglected and the rail pressure signal and fuel injection pattern are considered as exogenous inputs. As discussed earlier, IES and EIS modules are responsible for dynamic behavior of engine while the memory less ICP module is responsible for complex behavior of engine. The indexing sequence of pressure and temperature as well as gas flow rates is illustrated in Fig. 4. where T, P and X stands for absolute temperature, pressure and burnt gas fraction, respectively.

3.4. Intake and exhaust systems

IES comprises all the systems which participate in directing the air and emission flows. Three distinct paths are used to control the air and emission flow and their quality. In the proposed engine a VGT Turbocharger (TC) beside throttle valve is employed to control air pressure, in addition, an EGR valve is used to provide inlet air with desired EGR rate with the aim of decreasing NOx generation.

3.4.1. Turbocharger

The proposed engine employs a VGT type TC which its performance can be altered with variation of turbine blades angle. The TC comprises turbine, compressor and a common shaft which transfers the turbine generated power to compressor. Consequently, both compressor and turbine should be modeled using appropriate equations. The required power to increase the ideal gas pressure can be estimated using the following equation:

$$PW_c = \dot{m}_c c_p T_a \frac{1}{\eta_c}\left[\left(\frac{P_p}{P_a}\right)^{\frac{\gamma-1}{\gamma}} - 1\right] \quad (1)$$

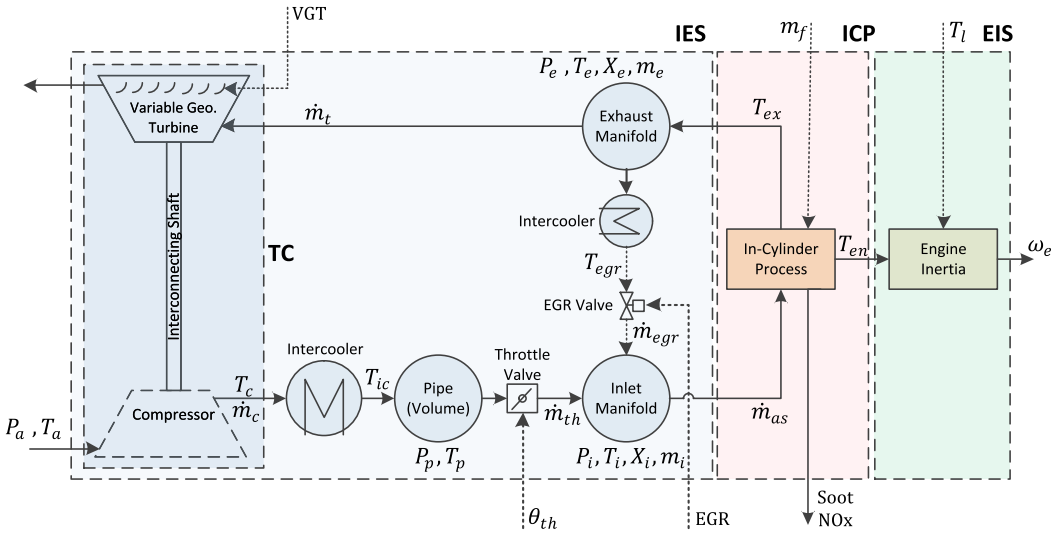

Fig. 4. The engine model architecture.

In which c_p is the gas specific heat in constant pressure, γ is specific heat ratio and η_c is the compressor efficiency. Compressing the inducted air will increase the gas temperature, which is modeled as follows:

$$T_c = T_a\left\{1+\frac{1}{\eta_c}\left[\left(\frac{P_p}{P_a}\right)^{\frac{\gamma-1}{\gamma}}-1\right]\right\} \tag{2}$$

Turbines use the gas enthalpy to generate required mechanical power; therefore, a decrease in the gas temperature occurs. The gas temperature after turbocharger can be modeled using the following equation:

$$T_t = T_e\left\{1-\eta_t\left[1-\left(\frac{P_t}{P_e}\right)^{\frac{\gamma-1}{\gamma}}\right]\right\} \tag{3}$$

where η_t is the turbine efficiency. In addition, the power generated by turbine can be calculated as follows:

$$PW_t = \dot{m}_t c_p T_e \eta_t\left[1-\left(\frac{P_t}{P_e}\right)^{\frac{\gamma-1}{\gamma}}\right] \tag{4}$$

Usually static maps are used to describe the compressor and turbine efficiencies and other performance parameters. The standard compressor maps report compressor efficiency and pressure ratio as a function of compressor rotational speed and mass flow rate. On the other hand, turbine standard maps demonstrate turbine mass flow rate and efficiency as a function of pressure ratio, turbine speed and VGT position.

The static maps developed for describing compressors operation usually report compressor efficiency in medium to high speed of compressor operation; as a result extrapolation methods are usually used for lower speeds. Standard methods of extrapolation usually fail to predict compressor efficiency in low TC speeds [25,26]. The same problem exists for turbine. Dinescu and Tazerout used dimensional analysis to overcome this problem [25]. They defined flow coefficient (ϕ), circumferential Mach number (M) and isentropic work coefficient (ψ) as non-dimensional numbers to extrapolate compressor maps. ϕ is defined as the ratio of flow velocity V to blade tip speed U.

$$\phi = \frac{V}{U} = \frac{\frac{\dot{m}_{c,cor}}{\rho\pi(D/2)^2}}{\omega_{tc,cor}(D/2)} \tag{5}$$

where $\dot{m}_{c,cor}$ is the corrected compressor mass flow rate, ρ is the air density in the up-stream of compressor, $\omega_{tc,cor}$ is the corrected compressor speed and D is the diameter of compressor blade. On the other hand, circumferential M and ψ are defined as follows:

$$M = \frac{\frac{\dot{m}_{c,cor}}{\rho\pi(D/2)^2}}{\sqrt{\gamma R T_a}} \tag{6}$$

$$\psi = \frac{c_p T_a\left(pr^{\frac{\gamma-1}{\gamma}}-1\right)}{\frac{[\omega_{tc,cor}(D/2)]^2}{2}} \tag{7}$$

In addition, they introduce Blade Speed Ratio (BSR) as the non-dimensional factor, which can be used in extrapolation of turbine maps. The BSR is defined as the ratio of blade tip speed U to isentropic nozzle flow C:

$$bsr = \frac{U}{C} = \frac{\omega_{tc,cor}(D/2)}{\sqrt{2c_pT_a\left(1-p_{r,t}^{\frac{\gamma-1}{\gamma}}\right)}} \tag{8}$$

where D is the turbine blade diameter and $p_{r,t}$ is the pressure ratio across the turbine. Using these non-dimensional factors, the behavior of turbocharger can be modeled in whole operational range. Using the mentioned non-dimensional parameters, the functions with extrapolating capability are developed which are seen in Table 1.

The standard functions data can be converted to non-dimensional compatible form. The generated non-dimensional data can be formulated by multi-dimensional surface fitting techniques.

TC shaft is the interconnecting component, which transfers the turbine-generated power to compressor. The differences of power accelerate/decelerate the TC shaft according to Euler equation as follows:

$$\dot{\omega}_{tc} = \frac{PW_t - PW_c}{\omega_{tc} I_{tc}} \tag{9}$$

where I_{tc} is the TC blades and interconnecting shaft rotational inertia.

3.4.2. Manifold processes

An influential phenomenon on engine dynamics is the manifold processes. The manifolds are modeled using a combination of continuity and energy equations. Lumped transient modeling is used to simulate pressure and temperature variations in the manifolds. The effect of wall heat losses and wave propagation in manifolds are neglected and the accumulated gas is assumed to be ideal gas. The pressure in input manifold is calculated by following equations:

$$\dot{P}_i = \frac{\gamma R}{V_i}(T_p\dot{m}_{th} + T_{egr}\dot{m}_{egr} - T_i\dot{m}_{as}) \tag{10}$$

In which γ is the air specific heat ratio, R is the gas constant, V_i is the inlet manifold volume and $\dot{m}_{as}$ is the engine aspirated mass flow rate which is derived from ICP model. The other parameters and related indices are shown in Fig. 4. Usually interpolated models are used for modeling the volumetric efficiency based on which aspirated mass flow rate is calculated. In this paper, the cyclic simulation is used to calculate the aspirated mass flow rate based on different boundary conditions on cylinder. Also, the exhaust manifold pressure is derived using the following differential equation:

$$\dot{P}_e = \frac{\gamma R}{V_e}(T_{ex}\dot{m}_{as} - T_e(\dot{m}_{egr} + \dot{m}_t)) \tag{11}$$

where V_e is the exhaust manifold volume and T_{ex} is the exhaust gas temperature which will be calculated from ICP model. The connecting pipe between intercooler and throttle valve also operates as an accumulating volume. Its pressure can be found from the following equation:

$$\dot{P}_p = \frac{\gamma R}{V_p}(T_{ic}\dot{m}_c - T_p\dot{m}_{th}) \tag{12}$$

In which, V_p is the volume of pipe and connections between compressor and throttle valve. The accumulated mass in manifolds and pipes can be calculated using continuity equation as follows:

$$\frac{d}{dt}m_i = \dot{m}_{th} + \dot{m}_{egr} - \dot{m}_{as} \tag{13}$$

$$\frac{d}{dt}m_e = \dot{m}_{as} + \dot{m}_{egr} - \dot{m}_t \tag{14}$$

Table 1
Extrapolating non-dimensional functions.

Standard Form	Non-Dimensional Form
$pr = f_1(\omega_{tc}, \dot{m}_{c,cor})$	$\phi = g_1(\psi, M)$
$\eta_c = f_2(\omega_{tc}, \dot{m}_{c,cor})$	$\eta_c = g_2(\phi, M)$
$\dot{m}_{t,cor} = f_3(pr, VGT)$	$\dot{m}_{t,cor} = g_3(pr, VGT)$
$\eta_t = f_4(\omega_{tc}, VGT)$	$\eta_t = g_4(bsr, VGT)$

$$\frac{d}{dt}m_p = \dot{m}_c - \dot{m}_{th} \tag{15}$$

Having the pressure and accumulated mass in each manifold, the temperature can be found using ideal gas state equation as follows:

$$T_i = \frac{V_i}{Rm_i}P_i \tag{16}$$

$$T_e = \frac{V_e}{Rm_e}P_e \tag{17}$$

$$T_p = \frac{V_p}{Rm_p}P_p \tag{18}$$

3.4.3. Throttle valve modeling

The diesel engines' generated torque is controlled directly by injected fuel mass, so in contrary to gasoline engine no throttle valve is used to control the generated power. Where low level of mechanical power is needed, the AFR increases, which in turn increases the generated NOx significantly. That is why modern diesel engines are equipped with throttle valve. Usually orifice air mass flow rate equation is used to model the mass flow across the throttle valve. In this paper, the model developed by Hendricks et al. is employed [27]. Hendricks suggested that air mass flow rate across the throttle can be modeled using two parallel orifices as follows:

$$\dot{m}_{th} = \frac{P_p}{\sqrt{RT_p}}\beta_1(\theta_{th}) \times \beta_2(p_{r,th}) \tag{19}$$

In which $p_{r,th}$ is the pressure ratio across the throttle valve and θ_{th} is throttle valve opening angle. β_1 function is defined as follows:

$$\beta_1(\theta) = b_0 + b_1\cos(\theta_{th}) + b_2\cos^2(\theta_{th}) \tag{20}$$

b_0, b_1 and b_2 are found from experimental tests. Also β_2 is defined as:

$$\beta_2(\theta) = \begin{cases} \frac{1}{0.74}\sqrt{p_{r,th}^{0.4404} - p_{r,th}^{2.3086}}, & p_{r,th} \geqslant 0.4125 \\ 1, & p_{r,th} < 0.4125 \end{cases} \tag{21}$$

3.4.4. Intercooler modeling

The temperature of air downstream compressor intercooler is modeled using the heat exchanger efficiency as follows:

$$T_{ic} = \eta_{ic,c}T_{cool} + (1 - \eta_{ic,c})T_c \tag{22}$$

where $\eta_{ic,c}$ is the compressor heat exchanger efficiency and is derived using experimental tests and T_{cool} is the coolant fluid temperature. In addition, the temperature of cooled recycled gas is calculated as follows:

$$T_{egr} = \eta_{ic,egr}T_{cool} + (1 - \eta_{ic,egr})T_e \tag{23}$$

In which, $\eta_{ic,egr}$ is the EGR heat exchanger efficiency.

3.4.5. EGR modeling

EGR modeling is comprised of calculating the exhaust gas flow through the EGR valve and calculation of EGR rate in inlet manifold. Standard orifice flow model is used to calculate the EGR flow through the valve as follows:

$$\dot{m}_{egr} = \frac{A_r(x_{egr})P_e}{\sqrt{RT_{egr}}}\sqrt{\frac{2\gamma}{\gamma - 1}\left(p_{r,egr}^{2/\gamma} - p_{r,egr}^{(\gamma+1)/\gamma}\right)} \tag{24}$$

In which x_{egr} is the normalized valve opening signal, A_r is the opening area of EGR valve and $p_{r,egr}$ is the pressure ratio across the valve and is calculated based on following equation:

$$p_{r,egr} = max\left(\frac{P_i}{P_e}, \left(\frac{2}{\gamma + 1}\right)^{\frac{\gamma}{\gamma-1}}\right) \tag{25}$$

EGR rate can be found from species continuity equation for burned gas [28]. In this paper the EGR rate is defined as the burned gas fraction in inlet manifold. The burned gas is conducted to inlet manifold from exhaust manifold using the EGR valve. Assuming uniform accumulated mass in both exhaust and inlet manifolds, the burned gas trapped in inlet manifold can be estimated as follows:

$$\frac{d}{dt}m_{x,i} = X_e\dot{m}_{egr} - X_i\dot{m}_{as} \tag{26}$$

In which $m_{x,i}$ is the mass of burned gas in inlet manifold and X_i and X_e are the burned gas fractions in inlet and exhaust manifolds respectively, X_i (EGR rate) is defined as follows.

$$X_i = \frac{m_{x,i}}{m_i} \tag{27}$$

It should be noted that in lean operation, some fresh air might exist in exhaust manifold; consequently, the EGR valve opening cannot increase the burned gas fraction in inlet manifold. A simple model is used for predicting the amount of unburned air in exhaust gas. It is assumed that in lean operation, the injected fuel burns as much air as demanded to provide a stoichiometric combustion and the remaining air will leave the cylinder unburned, consequently the mass flow rate of fresh air to exhaust manifold ($\dot{m}_{ex,a}$) is estimated as follows:

$$\dot{m}_{ex,a} = \dot{m}_{as}(1 - X_i) - \dot{m}_f \times 14.7 \tag{28}$$

On the other hand, in the rich regime, all the available air will be consumed and no fresh air enters the exhaust manifold i.e. $\dot{m}_{ex,a} = 0$ in rich operation. The mass of unburned air in exhaust manifold is estimated as follows:

$$\frac{d}{dt}m_{a,e} = \dot{m}_{ex,a} - (1 - X_e)(\dot{m}_{egr} + \dot{m}_t) \tag{29}$$

The burned gas ratio in exhaust manifold is calculated using following equation:

$$X_e = \frac{m_e - m_{a,e}}{m_e} \tag{30}$$

3.5. In-cylinder process modeling

The ICP model is the core of our modeling scheme. Engine generated torque, exhaust emissions, volumetric efficiency (aspirated air mass flow to cylinder) and exhaust gas temperature are calculated based on engine cycle thermodynamic model. Since the cycle thermodynamic model is computationally complex and not suitable for dynamic modeling, ANN modeling tool is used instead. As many data sets are needed to model the in-cylinder process with desired level of accuracy, a validated model-based approach is employed to make adequate data to train a neural network. AVL-Boost as an engine modeling package is used to model the thermodynamic cycle of a 1.5L common rail light duty diesel engine. Fig. 5 shows the flow-work of our research. However, the detailed thermodynamic modeling is not stated here and the interested readers can be found the detailed modeling approach in [29].

3.5.1. Cycle modeling using AVL-Boost

AVL-Boost is a powerful thermodynamic simulation software which is able to model the engine cycles using schematic blocks. Modeling tools need some engine geometric and phenomenal properties to simulate engine performance better. Some geometrical and operational data are obtained using

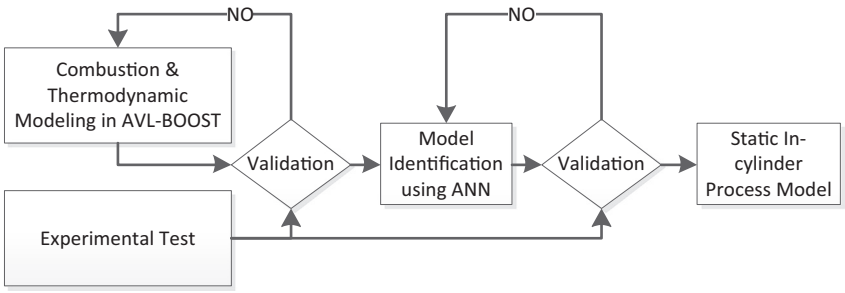

Fig. 5. The flow-work of in-cylinder model.

manufacturing data. Valve properties, injector specification and friction properties of engine are the most important specifications in our modeling. A major problem in engine modeling is estimating the friction of engine parts and pumping losses. Willans line is used to find the Friction Mean Effective Pressure (FMEP) in each engine speed.

3.5.2. Neural network modeling

3.5.2.1. Data generation. The developed model is used to generate required data for neural network development. About 3000 data is generated in whole possible engine operational points. Due to large input space (10 inputs) the factorial method would ends in too many data points. So the Sobol method is used to generate the desired data. Sobol method is a statistical method which obtains sequences in n-dimensional cube with low discrepancy [30]. In our research a 10 dimensions vector is considered as input data which is simply bounded between two minimum and maximum limits. The generated input data sets are used as inputs to the developed AVL-Boost model. For every set of data, 5 outputs are generated.

3.5.2.2. Neural network structure and training. Although the generated data covers the whole engine operational space, it is not sufficient for prediction of engine behavior in all of its operational conditions. So ANN as a powerful interpolator is used. Regarding the largeness of data dimensions and the number of data sets, an appropriate structure and training method should be used. Multi-Layer Perceptron (MLP) is used as a regular ANN structure. Due to large space of input and outputs and lack of data in comparison to whole operating range, there is high tendency to over-fit in training procedure. In order to avoid over-fitting and increasing the generalization of network, Bayesian regularization method is used for training the network. The Bayesian method is a probabilistic method which takes into account both the network architecture and estimation error while training. A sophisticated study on Bayesian training method is done by Bishop and Christopher [31] and also Lampinen and Vehtari [32].

Among five outputs, the emission outputs and specially soot shows different learning behaviors. The nonlinear behaviors of soot generation makes it difficult to train parameter. Due to different behavior of soot and NOx, a distinct network is employed to

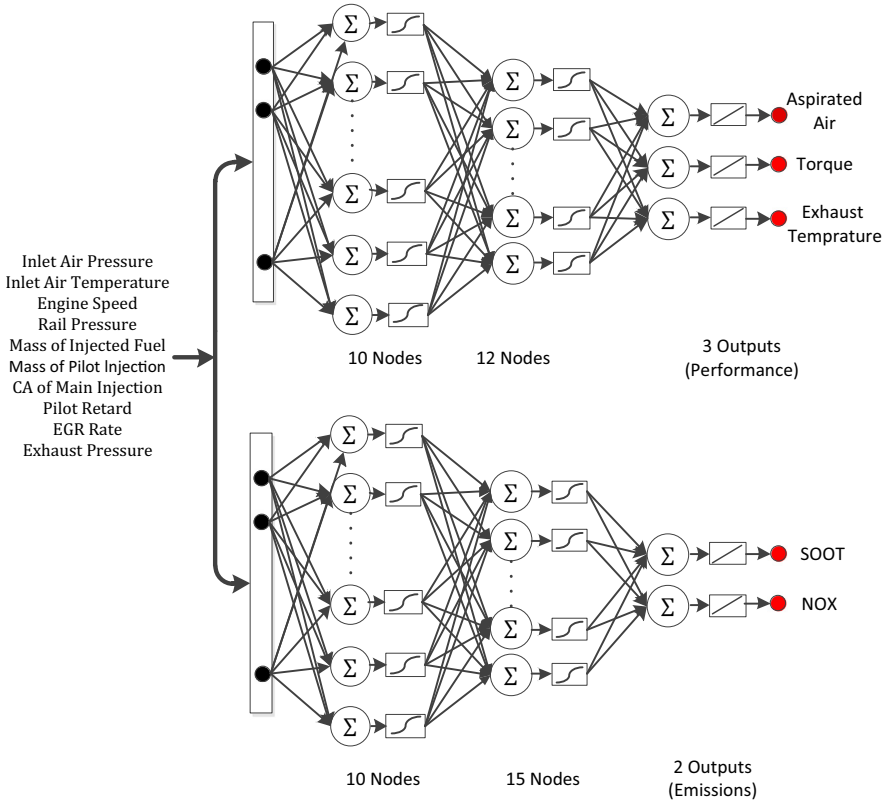

Fig. 6. Developed parallel MLP ANNs (Weights not shown on the connectors).

imitate the emissions behavior. The soot and NOx outputs have trained to network based on their pure mass (not brake specific emission generation). In order to be able to use these affective parameters as inputs for the network, two parallel neural networks are employed for modeling of all outputs as shown in Fig. 6. The first network is used to model torque, inducted mass and exhaust temperature while the second one is responsible for prediction of raw emissions.

As depicted in Fig. 6, for the first network a two layers ANN having 10 and 12 neurons in hidden layers is used, which is important to performance prediction i.e. torque, aspirated air and exhaust temperature. In the second network a two layer ANN with 10 and 15 nodes in hidden layers are employed due to more complex behavior of emission generation.

Every MLP structure is designed with two hidden layers and sigmoid activation functions for hidden layers and linear activation function for the output layers. The number of neurons in MLP structure is selected based on minimum error and calculation parameters.

3.6. Engine inertial modeling

The Euler equation is employed for modeling the engine inertial dynamics. The inertia of engine compromises the crankshaft, the equal reciprocal piston masses and other moving parts of engine. The rotational speed of engine is calculated using the following equation:

$$\dot{\omega}_{eng} = \frac{\tau_b - \tau_l}{I_{en}} \tag{31}$$

In which τ_b is the engine generated torque and τ_l is external load torque. τ_b is the generated net torque and is derived from ICP model. It should also be noted that the friction and pumping losses have been considered in ICP.

Table 2
The engine specifications.

Displaced volume	1497 CC
Number of cylinders	4
Stroke	82.5 mm
Bore	76 mm
Connecting rod	134.25 mm
Compression ratio	16.5:1
Number of valves per cyl.	4
Injection system	Common rail
Air boost system	VGT + intercooler

4. Results and discussion

4.1. Engine and turbocharger specifications

In this paper a 1.5L common rail turbocharged diesel engine is considered. The engine specifications are listed in Table 2.

Piezoelectric injectors with 8 holes (0.11 mm diameter) are used in the engine fuel injection system. Injector flow map is used to model the injection process.

Turbocharger is the other important component of engine, which is considered in engine dynamic modeling. As discussed earlier, a non-dimensional approach is employed to promote prediction capability of model to cover whole turbocharger operational space. The data are extracted from turbine and compressor map and converted to desired non-dimensional values. Matlab® Surface Fitting Tool™ is used to find the appropriate polynomial, which can best describe the relation between non-dimensional values. The non-dimensional functions which are used in compressor modeling are depicted in Fig. 7. It is seen that instead of $\phi = g_1(\psi, M)$ function which was already shown in Table 1, $\psi = g_4(\phi, M)$ is fitted due to better abilities to be fitted by polynomials. Then inverse function technique is used to derive desired function out of it.

The non-dimensional functions for turbine modeling are shown in Fig. 8.

As discussed earlier intercoolers are also modeled using heat exchanger equation as described in Eqs. (22) and (23). The heat exchanger efficiency is strictly depended to air mass flow rate through it. Using experimental data and curve fitting technique, a twin exponential function is derived which can best describe the dependence of intercooler efficiency to air mass flow rate (see Fig. 9).

4.2. Model execution properties

As discussed before the whole modeling can be taken into following parts: combustion modeling and dynamic modeling. For combustion modeling AVL-Boost is used. More than 3000 data sets are generated. The AVL-Boost employs an iterative solving procedure for a single cycle simulation for data generation purposes. The convergence criteria for simulation termination was set to 10 iterates. Every cycle simulation took about 25–30 s; altogether the data generation process took more than 24 h. Matlab® (R2010a)/Neural Network Toolbox is employed for generation and training of required ANN. On the other hand, the dynamic model is developed in Matlab® (R2010a)/Simulink® (ver. 7.5). The variable step solver of "ode15s" is used to simulate the model

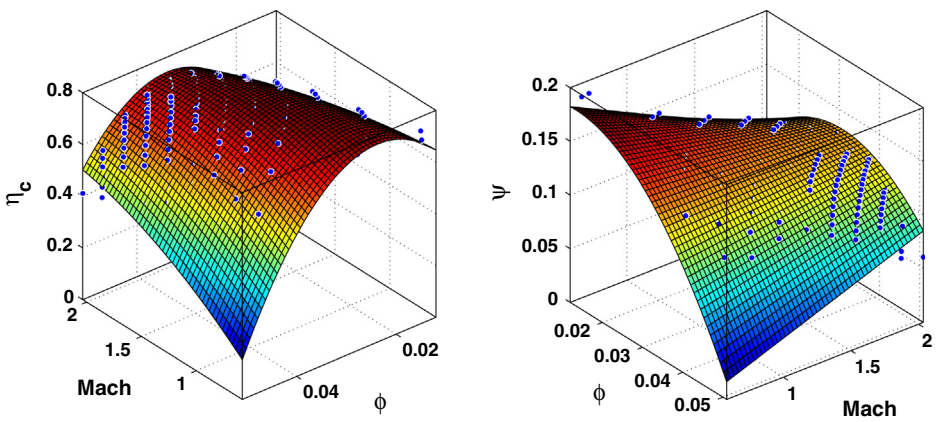

Fig. 7. Non-dimensional functions for compressor modeling.

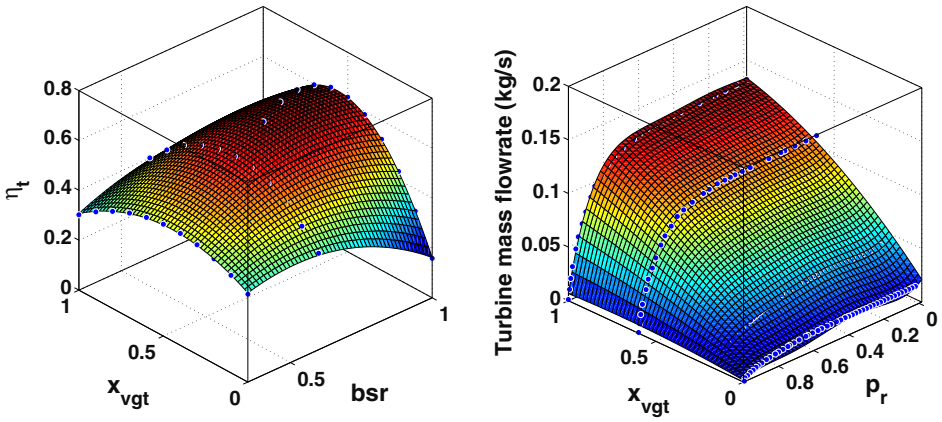

Fig. 8. Non-dimensional functions for turbine modeling.

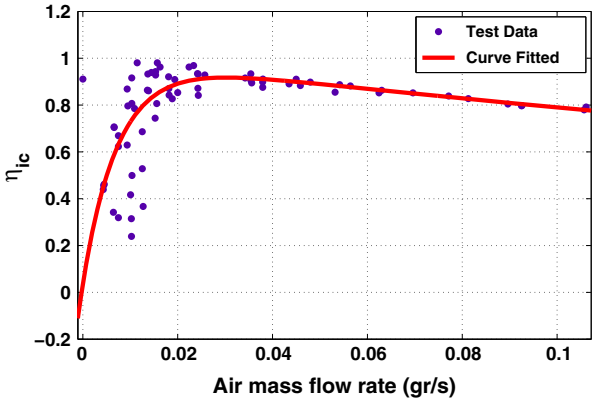

Fig. 9. Dependency of intercooler efficiency as a function of air mass flow rate.

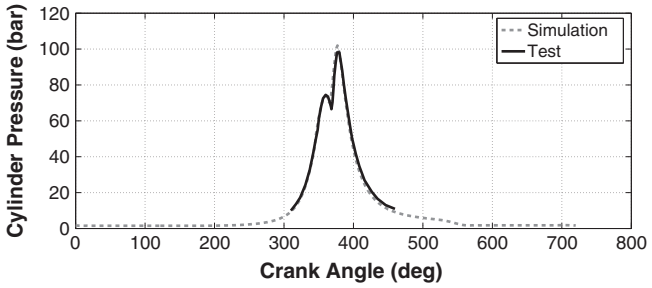

Fig. 10. Comparison of in-cylinder pressure vs. crank angle in full load operation, $RPM = 1500$ rpm, $p_{rail} = 1308$ bar, $EGR = 11\%$, $\theta_{inj} = 1.89°$ $BTDC$, $\Delta\theta_{pilot} = 22°$, $m_p = 1.92 \frac{mg}{cycle}$, $p_{in} = 1.43$ bar, $p_{out} = 1.88$ bar, $T_{in} = 19$ °C, $\phi = 0.95$.

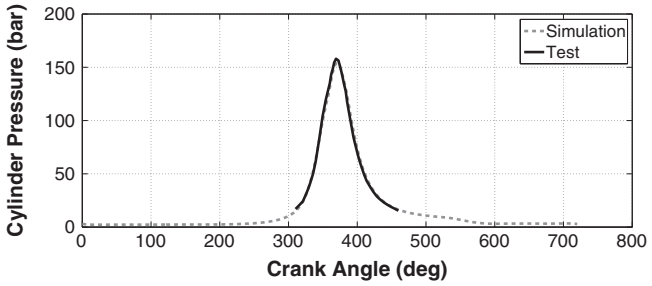

Fig. 11. Comparison of in-cylinder pressure vs. crank angle in full load operation, $RPM = 3500$ rpm, $p_{rail} = 1571$ bar, $EGR = 4\%$, $\theta_{inj} = 13°$ $BTDC$, $\Delta\theta_{pilot} = 42°$, $m_p = 2.32 \frac{mg}{cycle}$, $p_{in} = 2.32$ bar, $p_{out} = 3.90$ bar, $T_{in} = 46$ °C, $\phi = 0.91$.

due to its high simulation speed and it adequate accuracy in the simulation of this specified model. The simulation of engine operation for a 600 s procedure of variation of load and injection quantity takes about 5.64 s with 0.48 s for model initialization period. This simulation duration is for dedicated engine simulation without any controller applied to model.

4.3. Model validation

For model validation aims, the engine is tested both in static and transient modes. The static test data is used mainly to validate ICP model (combustion model) while transient data sets are used to validate the complete (dynamic model).

4.3.1. Combustion model validation

After model verification, the developed model is validated using a comparison between model outputs and test data. Both crank angle-based data and cyclic cumulative data i.e. torque and emissions are used for validation purposes. The combustion pressure profile is compared with model results. The pressure-crank angle data of engine is recorded using pressure sensors mounted on the engine cylinder head. The following figures show the comparison between experimental pressure data and model results.

As depicted in Figs. 10 and 11 the test results and simulation for engine operation in full load condition are in good agreement.

Another comparison is also done based on cyclic cumulative values. In order to better validate the model results, whole engine operating space is considered. Engine is tested in both part load and full load conditions; the comparison is done for torque generation, aspirated air, NOx and Soot generation in whole engine operating space. The errors in part load conditions are estimated based on comparison between model outputs and experimental data. The net errors in whole engine operation regime are 1.7%, 2.2%, 3.4% and 4.3% respectively for torque generation, aspirated air, NOx and soot generation.

4.3.2. Neural network evaluation

The results of training and performance of network is evaluated by calculating the error of network to untrained data sets and also using the comparison between experimental data and neural network results. About 2500 data sets are used for training network. 500 data sets remained for evaluation purposes. For evaluation of rational performance Eq. (32) is used:

$$er = \frac{\sum_{i=1}^{500} |m_i - t_i|}{\sum_{i=1}^{500} |t_i|} \times 100 \tag{32}$$

where m_i and t_i are the neural network result and AVL model value respectively. The results shows 2.4% error in modeling the aspirated air mass, 3.9% error in estimation of generated torque, 5.4% error in NOx amount, 5.8% error in Soot modeling and 2.2% error in prediction of exhaust temperature.

As stated earlier, all the results have errors lower than 6%. The inducted air and exhaust temperature have the least errors while torque and emissions have fairly acceptable errors. Also for better ANN evaluating, the results are compared with experimental data.

The comparison of full load data test, AVL model results and ANN model is done to check the validity of the models. Since the ANN model will be used in whole engine operating conditions, the validity of model should be considered in both full load and part load. The engine is tested under different full load and part load speeds and brake torque, aspirated air, NOx, soot, BSFC and exhaust gas temperature is considered and compared. The results show good agreement in both full load and part load. The results of AVL model and ANN model are compared with real data as depicted in Fig. 12.

The comparison of ANN model data and test data is also done in part load. The results show the contour of error percentage of different outputs in BMEP vs. engine speed plane as depicted in Fig. 13. The results show good agreement between model results and test data.

4.3.3. Dynamic model validation (step response)

The proposed dynamic modeling method (EMVM) is validated by comparison of both step response and frequency response of model results and test data. In this section, the step response data are employed to validate the dynamic model. The effect of main engine inputs such as injected fuel mass, engine load, EGR valve, throttle valve, VGT position, rail pressure and injection pattern on engine outputs are measured and compared with model results. The ambient condition (air pressure and temperature) are controlled to be in standard values both for model and experimental equipment.

The test result of injected fuel increase is shown in Fig. 14. The injected fuel is increased from 16 mg/cycle to 18 mg/cycle in constant engine load of 78 N m; the engine speed increases as well. However due to external load and engine inertia, the relatively slow engine speed increase is achieved. The lambda sensor shows decrease in λ which means a richer mixture is provided due to fuel increase. Due to engine dynamics i.e. slow engine speed increase an under-shoot is seen in λ which in turn lead to soot generation soon after injection value manipulation. Also, a relatively slow NOx decrease is seen after indicted fuel increase which is mainly due to decrease in λ value. The whole results show good agreement between experimental results and data ones, however there is a deviation in emission prediction, which is negligible.

To validate the load acceptance of model, a step load increase test is done on the engine, in constant engine operation condition; an increase in load stimuli is done using dynamometer from 60 N m to 75 N m. The test results and model prediction is illustrated in Fig. 15. As depicted, the engine speed decrease and settle down to new value. On the other hand, an overshoot is seen in lambda in the first moments of load acceptance. The main reason is turbocharger lag, i.e. engine speed decrease faster than turbocharger and causes pressure increase in inlet manifold; which

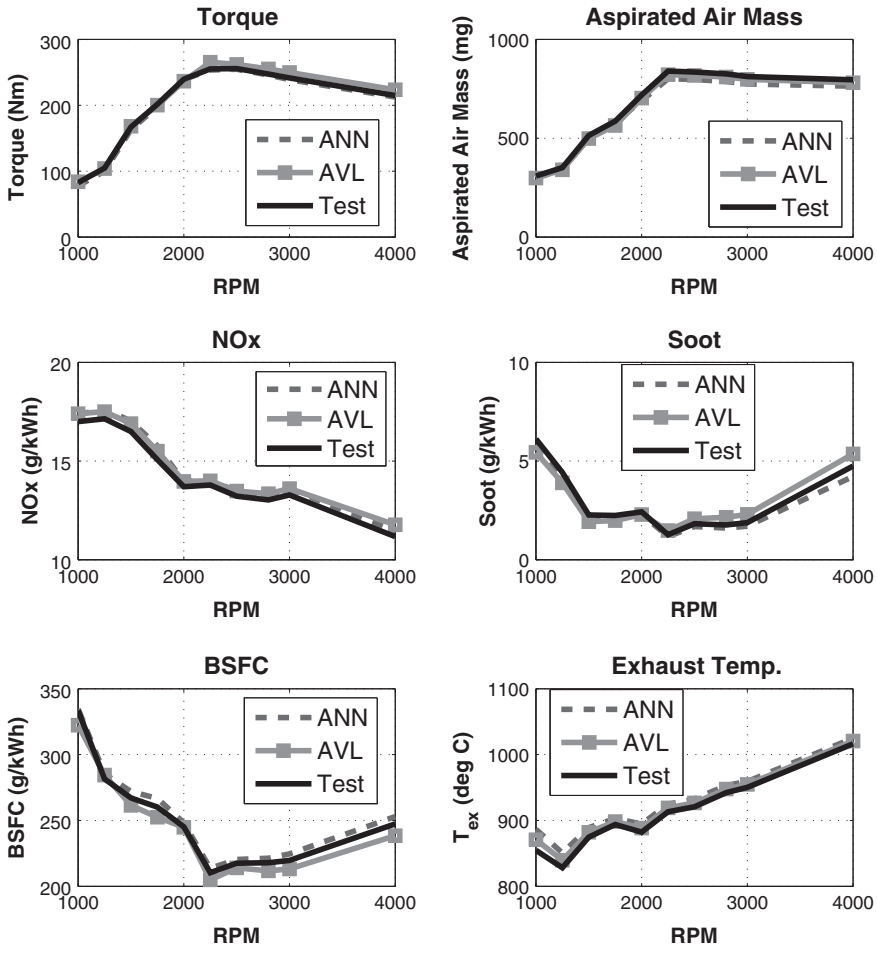

Fig. 12. Comparison of ANN, AVL model outputs and test results in full load.

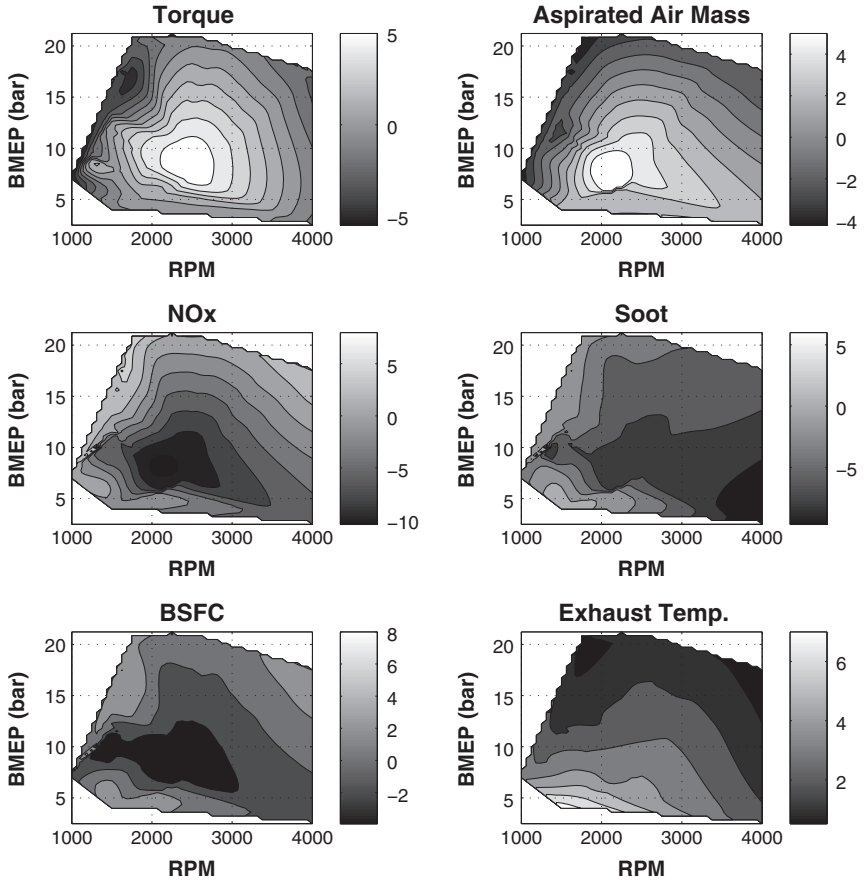

Fig. 13. Error percentage of ANN results and experimental data in part load.

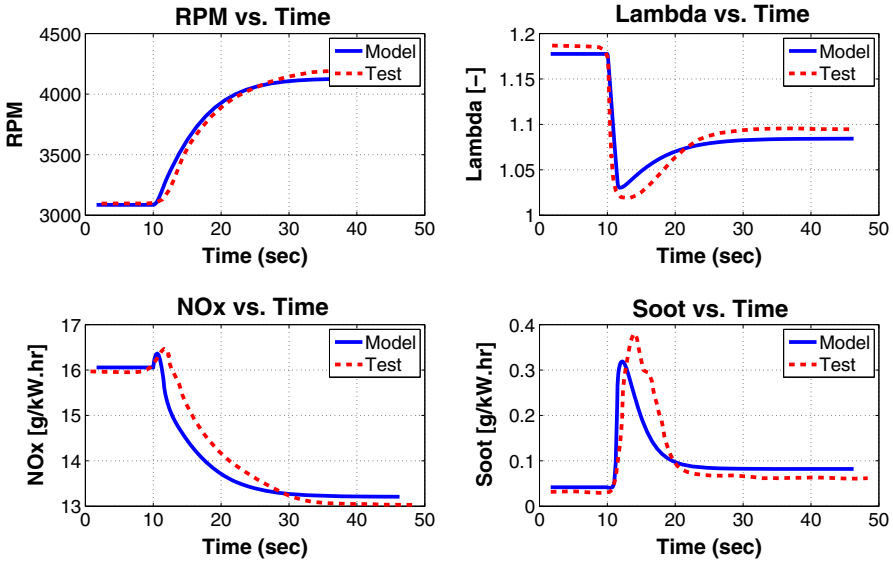

Fig. 14. Effect of a step increase in fuel injection from $m_f = 16\ \frac{mg}{cycle}$ to $m_f = 18\ \frac{mg}{cycle}$ in $t = 10$ s, $P_{rail} = 1100$ bar, $x_{vgt} = 80\%$, $x_{th} = 100\%$, $x_{egr} = 60\%$, $\theta_{inj} = 2^\circ$ $BTDC$, $\Delta\theta_{pilot} = 18^\circ$, $m_p = 1.2\ \frac{mg}{cycle}$, $\tau_b = 78$ N m.

in turn, increases the aspirated air mass for a while. As constant fuel is injected in this period, the mixture gets leaner in the first instants of load exertion and soon after, the richness will gradually disappear. The influence of load on lambda shows a non-minimum phase behavior. The increase of NOx is mainly due to decrease of lambda which will result in an increase of maximum cylinder temperature. The comparison of test and simulation results shows acceptable accordance.

The effect of EGR valve opening on engine operation is depicted in Fig. 16. The EGR valve is widely open from 20% to 80% in the 10th second of test. The described stimuli will end to increase in EGR rate in a relatively fast manner. As some amount of the

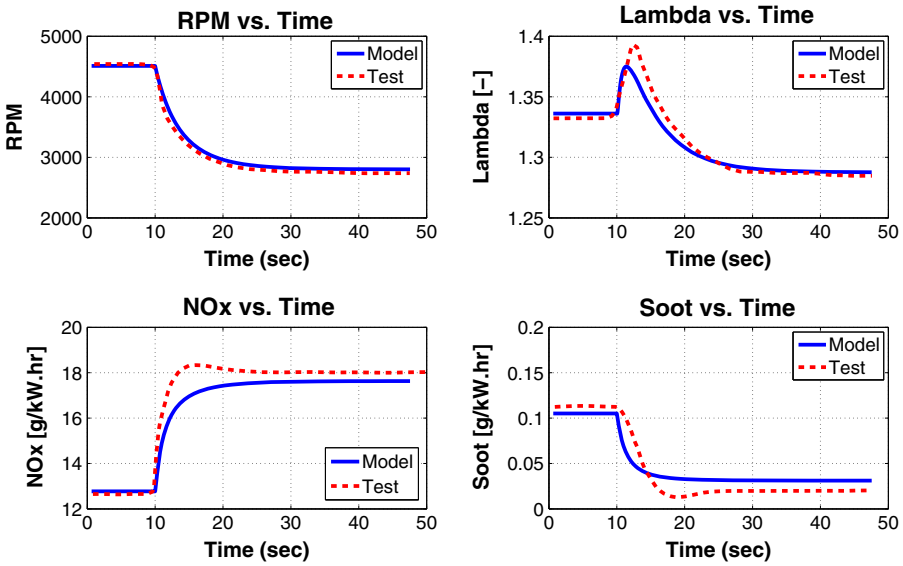

Fig. 15. Effect of a step increase in external load torque from 60 N m to 75 N m in $t = 10$ s, $P_{rail} = 1100$ bar, $x_{vgt} = 80\%$, $x_{th} = 100\%$, $x_{egr} = 50\%$, $\theta_{inj} = 2^\circ$ *BTDC*, $\theta_{pilot} = 18^\circ$, $m_p = 1.35\ \frac{mg}{cycle}$, $m_f = 18\ \frac{mg}{cycle}$.

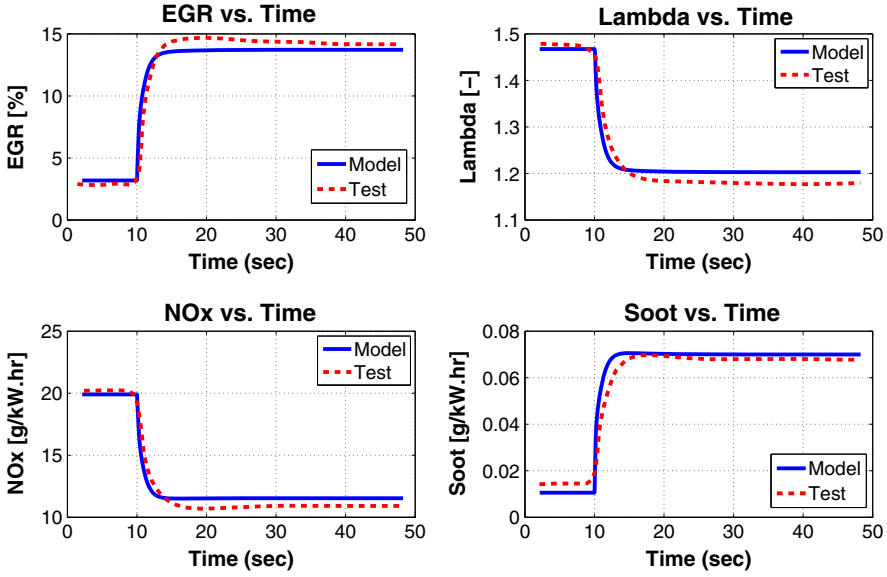

Fig. 16. Effect of a step increase in EGR valve opening from 20% to 80% in $t = 10$ s, $P_{rail} = 1100$ bar, $x_{vgt} = 80\%$, $x_{th} = 100\%$, $\theta_{inj} = 2^\circ$ *BTDC*, $\Delta\theta_{pilot} = 18^\circ$, $m_p = 1.1\ \frac{mg}{cycle}$, $m_f = 15\ \frac{mg}{cycle}$, $\tau_b = 75$ N m.

available air in inlet manifold is replaced by burned gas, the lambda decreases in a comparable speed to EGR rate increase. On the other hand, due to increase of EGR rate, the NOx production rate decreases while soot generation increases.

Modern diesel engines are equipped with VGT turbochargers to better control the inlet manifold pressure to desired values. Inlet manifold pressure influences engine parameters in different manners; engine torque, emissions and even EGR rate is highly affected by turbocharger blade angle. The dynamics of turbocharger besides engine inherent dynamics, results in complicated behavior of engine. The less opening of VGT would result to pressure increase in inlet manifold due to increase of turbine efficiency. The responses of engine to VGT opening decrease from 60% to 30% is depicted in Fig. 17. The engine speed shows a non-minimum phase behavior in response to VGT angle, i.e. while decrease the VGT opening engine speed shows a decrease in primitive moments, after which it increase to a limited value. Turbocharger speed increases in response to VGT opening decrease. This leads to inlet manifold pressure increase. NOx is a little increased while soot is mainly decreased due to inlet pressure boost. The non-minimal phase behavior of NOx is affected by EGR variation due to inlet manifold pressure change.

Diesel engines are not typically equipped with throttle valve; instead, fuel injection is employed to control the engine torque. In higher engine speeds and full load condition, less EGR rates are available due to high inlet manifold pressure which decreases the tendency of exhaust burnt gas to flow from exhaust manifold to inlet manifold. Throttle valves are used to decrease the inlet manifold pressure and increase the EGR rate. A Multi-Input Multi-Output (MIMO) controller is developed to control both pressure and EGR rate using VGT, EGR valve and Throttle valve actuators. The model is validated using experimental data which is

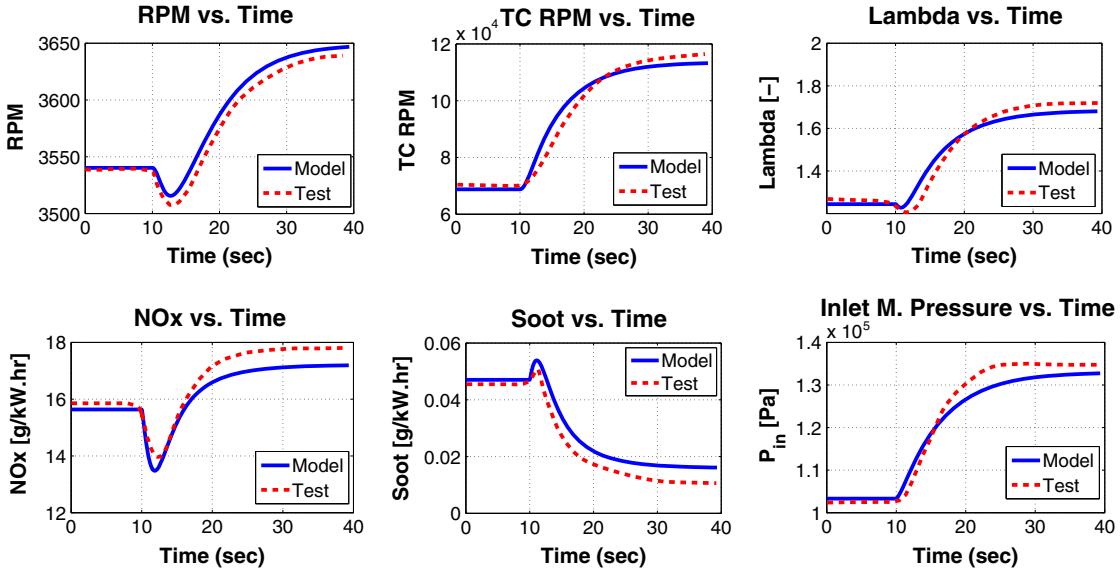

Fig. 17. Effect of a step decrease in VGT blade position from 60% to 20% in $t = 10$ s, $P_{rail} = 1100$ bar, $x_{egr} = 50\%$, $x_{th} = 100\%$, $\theta_{inj} = 2^\circ$ *BTDC*, $\Delta\theta_{pilot} = 20$ *BTDC*, $m_p = 1.1\ \frac{mg}{cycle}$, $m_f = 15\ \frac{mg}{cycle}$, $\tau_b = 75$ N m.

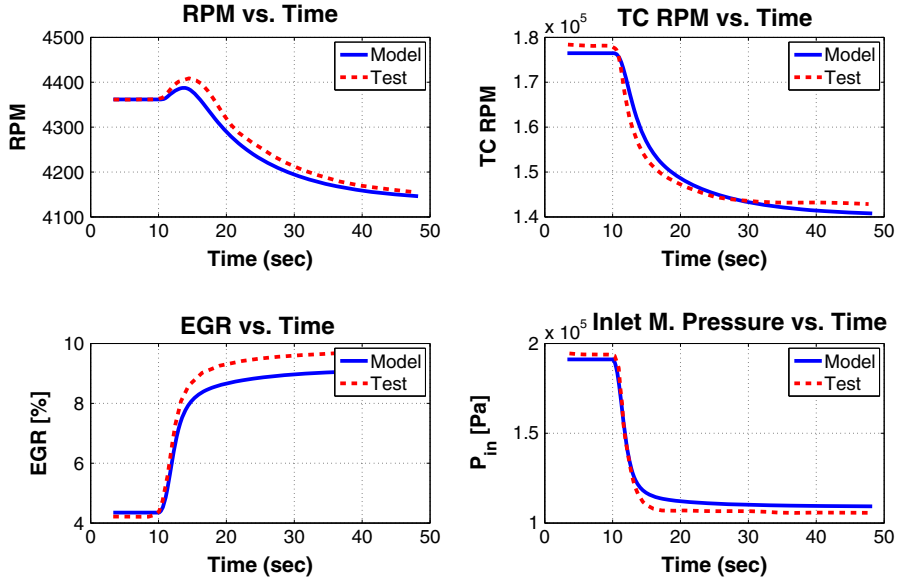

Fig. 18. Effect of a step decrease in Throttle valve from 100% to 30% in $t = 10$ s, $P_{rail} = 1400$ bar, $x_{egr} = 30\%$, $x_{vgt} = 20\%$, $\theta_{inj} = 2^\circ$ *BTDC*, $\Delta\theta_{pilot} = 13^\circ$, $m_p = 1.35\ \frac{mg}{cycle}$, $m_f = 18\ \frac{mg}{cycle}$, $\tau_b = 75$ N m.

obtained by a VGT actuator step test; the comparison results are illustrated in Fig. 18. The engine RPM and turbocharger speed shows a slow decreasing trend while a sharp decrease in inlet manifold is seen due to decreasing the opening area of throttle valve. The decrease in throttle valve opening results in increasing the flow loss in air induction path which in turn decreases the manifold pressure; as a result more exhaust gas is inducted to inlet manifold in fix EGR valve opening which in turn increase the EGR rate from 4% to about 9%. The comparison of simulation results with experimental data shows good agreement between model and real data.

Rail pressure is another important factor which can affect on emissions of engine to some extent in a relatively fast manner. The results of variation of fuel rail on engine emissions are shown in Fig. 19. In both cases a fluctuation in emission production rate is seen which is due to effects of rail pressure on engine speed. It should be noted that since the injection pressure can affect torque generation the engine speed is varied in constant load test procedure. As depicted in Fig. 19, the higher inlet manifold pressures increase NOx while decrease the soot. The better fuel atomization will increase the mixing process which in turn will make a more uniform mixture in sense of AFR. The result is decrease in soot production. On the other hand, the better mixing results in temperature increase, which will produce more nitrogen radicals. The availability of nitrogen radicals will increase the NOx generation rate. Also increasing the injection pressure will increase the part of fuel which is injected in premixed combustion phase that is usually the hottest part of diesel combustion. A comparison between

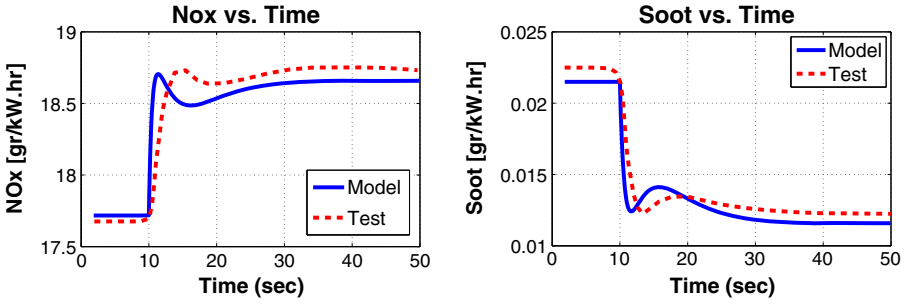

Fig. 19. Effect of a step increase in rail pressure from 900 bar to 1300 bar in $t = 10$ s, $x_{egr} = 40\%$, $x_{vgt} = 40\%$, $x_{th} = 100\%$, $\theta_{inj} = 2^\circ$ *BTDC*, $\Delta\theta_{pilot} = 13^\circ$, $m_p = 1.2\ \frac{mg}{cycle}$, $m_f = 16\ \frac{mg}{cycle}$, $\tau_b = 75$ N m.

test data and simulation results shows a delay in test result while being compared to real data which is mainly due to not modeling the rail pressure control module in the model.

Injection pattern i.e. main and pilot injection timing are two main effective parameters which can affect engine emission to high extent. In order to validate the model, a two-step test is done on the engine. In the first step, the main injection timing is advanced from 1° ATDC to 5° BTDC in the 10th second of the test, after which an advance in pilot injection in occurred from 15° BTDC to 30°BTDC in 50th second. The results are illustrated in Fig. 20. The results show good agreement between test and model. It's also shown that injection timing can rapidly affect the engine emission.

4.3.4. Dynamic model validation (frequency response)

However, the step response is useful in validation of dynamic models; frequency response comparison – where possible- will help us to validate the model in its whole frequency range for specific operating points. Since the model is developed in Matlab Simulink®, it is possible to derive the frequency response between

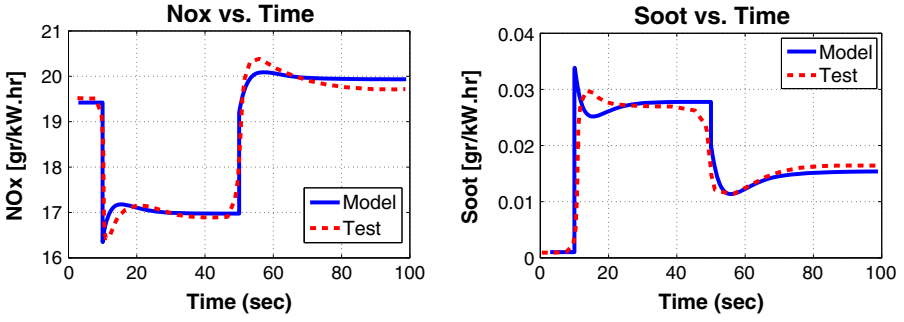

Fig. 20. Effect of a step advance in main injection timing from $\theta_{inj} = 5$ *BTDC* to $\theta_{inj} = 1$ *ATDC* in $t = 10$ s and advancing pilot injection timing from $\theta_{inj} = 15^\circ$ *BTDC* to $\Delta\theta_{pilot} = 15^\circ$ in $t = 50$ s, $x_{egr} = 40\%$, $x_{vgt} = 40\%$, $x_{th} = 100\%$, $m_p = 1.2\ \frac{mg}{cycle}$, $m_f = 16\ \frac{mg}{cycle}$, $\tau_b = 80$ N m.

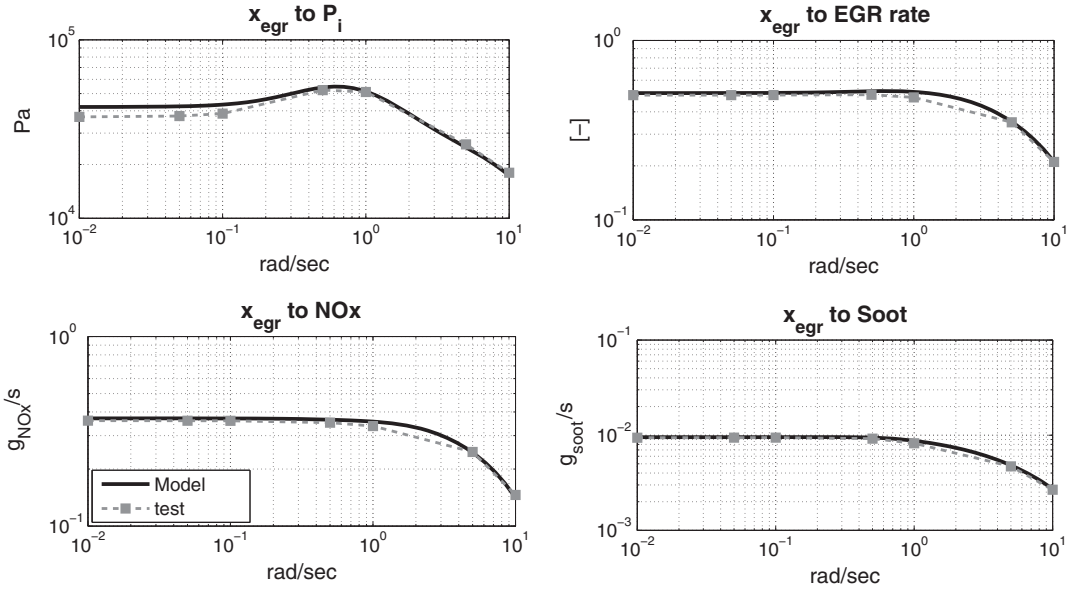

Fig. 21. The comparison of frequency responses of EGR valve variation on relevant states, *RPM* = 3000 rpm, $P_{rail} = 1550$ bar, $x_{vgt} = 6\%$, $\theta_{inj} = 10.6^\circ$ *BTDC*, $\Delta\theta_{pilot} = 12^\circ$, $m_p = 2\ \frac{mg}{cycle}$, $m_f = 25.6\ \frac{mg}{cycle}$, $\tau_b = 145$ N m.

any desired input and output. On the other hand, sinusoidal stimuli with defined frequency and limited amplitude are used as inputs and relevant outputs are measured to find the relative amplitude of output signal to input signal. In this comparison, the engine main dynamic inputs (EGR valve position and VGT blade position) altogether with injection mass are considered for test. The sinusoidal inputs with frequency of 0.01, 0.05, 0.1, 0.5, 1, 5 and 10 rad/s are used to test the engine. Since the whole model is nonlinear, the test should be done for a specific operating point, where it is possible to linearize the model around it. The emissions in following result are measured in mass flow rate of g/s rather than the brake specific generation rate.

The results of comparison of frequency response of EGR valve position of inlet manifold pressure, EGR rate and emissions are depicted in Fig. 21. The test has been done in 3000 rpm with 60% load. The result of tests shows that the test data and model data are in agreement in both low frequency and high frequencies. The low frequency proximity confirms that the steady state error should not be significant in step response test.

In order to study the effects of VGT blade position on engine operation; the frequency response between it and inlet manifold pressure, turbocharger speed and emissions are considered as depicted in Fig. 22. The test has been done in 2500 rpm and 80% load. The comparison between test and model results shows that the responses are in acceptable agreement. The lower frequencies in emission relevant have some meaningful difference that shows a steady state error in step response.

The matching between turbocharger speed and inlet manifold pressure is good in lower frequencies, which shows that the proposed method of turbocharger modeling can predict the turbine

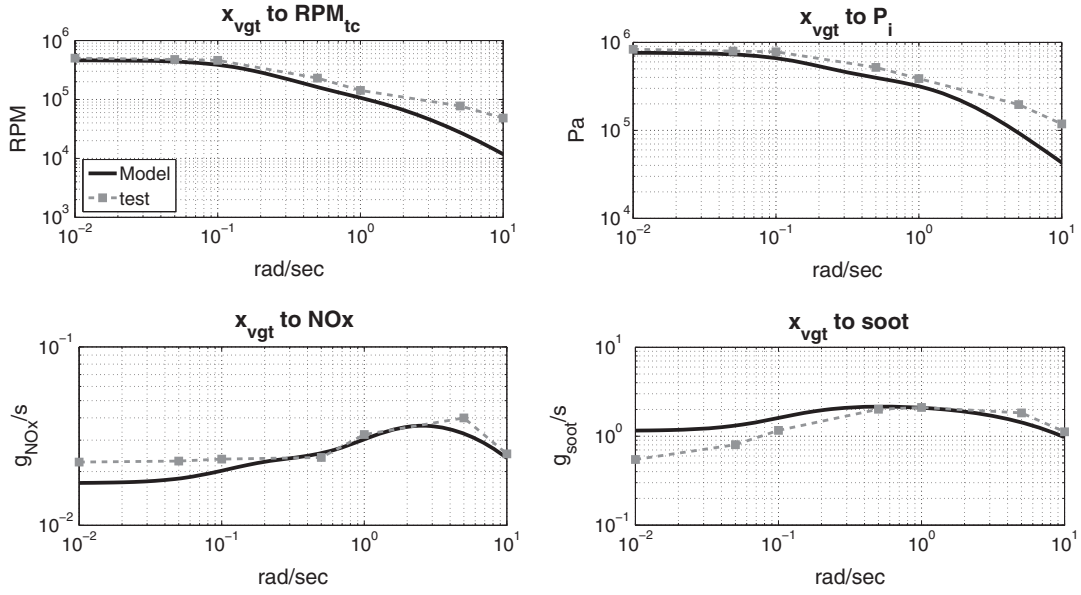

Fig. 22. The comparison of frequency responses of VGT position variation on relevant states, $RPM = 2500$ rpm, $P_{rail} = 1550$ bar, $x_{egr} = 23\%$, $\theta_{inj} = 6.58^\circ$ $BTDC$, $\Delta\theta_{pilot} = 10^\circ$, $m_p = 2.2\ \frac{mg}{cycle}$, $m_f = 33\ \frac{mg}{cycle}$, $\tau_b = 194$ N m.

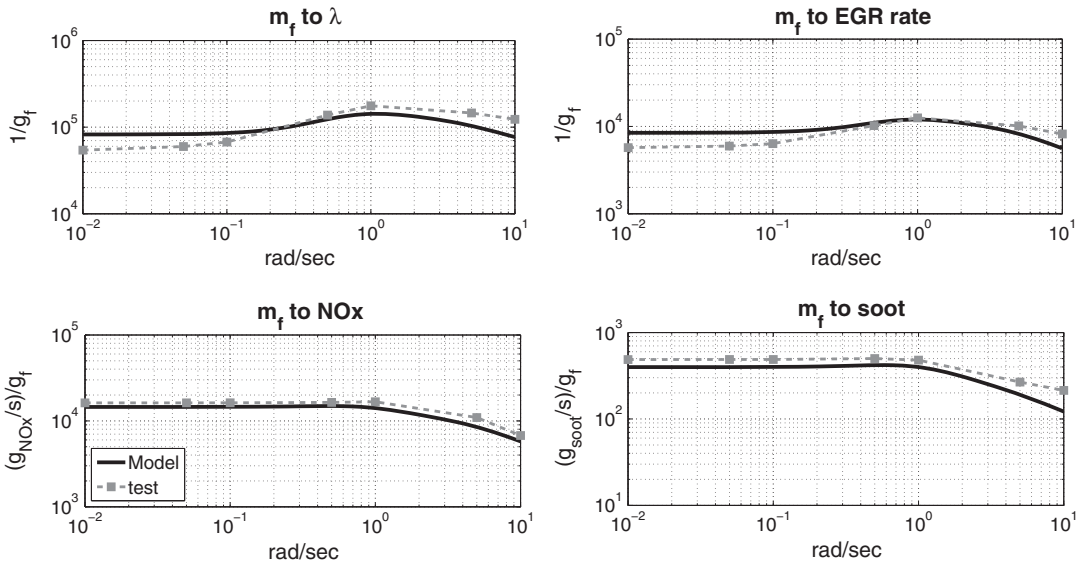

Fig. 23. The comparison of frequency responses of main injection variation on relevant states, $RPM = 4000$ rpm, $P_{rail} = 1600$ bar, $x_{vgt} = 10\%$, $x_{egr} = 34\%$, $\theta_{inj} = 15^\circ$ $BTDC$, $\Delta\theta_{pilot} = 23^\circ$, $m_p = 2.5\ \frac{mg}{cycle}$, $\tau_l = 121$ N m.

and compressor efficiency and mass flow well enough. On the other hand, it diverges in higher frequencies, which is mainly due to unmolded dynamics and specially the friction of turbocharger interconnecting shaft.

The dynamic influences of injection mass on lambda, EGR rate and emissions are also studied and the results are shown in Fig. 23. The comparison of model outputs with experimental data shows that they are in good agreement. The result shows a deviation in lower frequencies in both lambda and EGR rate frequency responses. The emissions are well modeled in dynamic operation.

5. Conclusion

The extended mean value model (EMVM) for control-oriented modeling of internal combustion engines is investigated based on block oriented modeling (BOM) concept. EMVM concept increases the capability of conventional MVMs in prediction of engine raw emissions and performance in transient regimes. The proposed model is able to predict the influences of main/pilot injection and timing, EGR valve position, VGT blade angles and throttle valve on brake torque, BSFC, soot and NOx in transient regimes. The specifications of EMVM in both accuracy and fast running aspects make it appropriate for model-based control development and real time applications. The BOM is a systematic point of view, which assumes the whole nonlinear dynamic systems to be composed of relatively simple dynamic systems coupled with high nonlinear semi-static systems.

The BOM concept is consistent with engine essence. The engine behavior is assumed to be associated with some distinct subsystems containing Inlet and Exhaust System (IES), Engine Inertial Systems (EIS), In-Cylinder Process (ICP) and Fuel Delivery System (FDS). All the sub-systems are naturally dynamic, but for modeling aims, the fast dynamic systems (ICP and FDS) are considered as semi-static systems. The ICP is the core of engine model and contains the complex combustion and gas exchange processes meanwhile it is responsible for prediction of performance and raw emissions. Due to complexity of combustion process, usually high computational burden models with iterative solution methods are used, which increase the time of simulation to high extend and make it inappropriate for control-oriented and real-time simulation. The combustion model is usually implemented in MVM using look-up tables, interpolated algebraic equation or crank angle based models. The tabulated data and interpolated equation methods are rapid but they have rarely been considered for modeling the emissions due to level of inaccuracy in emission modeling. Application of steady state data into MVM leads to inefficient models, which cannot predict the emissions with desired accuracy in transient modes; usually correction factors are used to compensate for transient prediction errors. On the other hand the number of inputs to combustion is limited which is not favorable for today control demands. In some models, the thermodynamic modeling coupled with chemical reaction models has been implemented in MVM models. Unfortunately, this type of modeling is computationally inconsistent with real time applications and makes the model too slow to run for control purposes. In this paper, ANN is employed to imitate the result of ICP modeling instead of using iterative solutions. Two parallel ANNs with two layers in each stage is trained offline and finally implemented in the main engine model. One of them is used for prediction of performance and the other is responsible for emission prediction. The Bayesian training method is used for overcoming the overfitting problem. The application of ANN decreases the time of modeling from 25 s/cycle to the order of 50 μs for running an ANN while retained the accuracy of model. The IES system contains the manifold phenomena and turbocharger dynamics. Both the mass and energy balance equations are used to model the dynamic process involved with the IES. Due to influences of EGR rate on engine emissions, the dynamic of burned gas fraction in both inlet and exhaust are considered using the mass balance for species. The developed model is validated in both steady and transient regimes. A test setup is used to derive the experimental data for validation task. The results of steady tests shows 2.4% error in modeling the aspirated air mass, 3.9% in estimation of generated torque, 5.4% in NOx amount, 5.8% in soot modeling and 2.2% in prediction of exhaust temperature. The transient validation is carried out both with step responses and frequency response. The comparison of experimental data with model outputs shows good agreement between them. The duration of model execution for running the model with limited white band noise signals applied on model inputs is less than 5 s for a 600 s simulation, which is favorable for real time application.

References

[1] Hafner Michael, Jost Oliver, Isermann Rolf. Mechatronic design approach for engine management systems. Mechatronics 2002;12:1035–46.
[2] Nikzadfar Kamyar, Shamekhi Amir H. More than one decade with development of common-rail diesel engine management systems: a literature review on modelling, control, estimation and calibration. Proc Inst Mech Eng, Part D: J Automob Eng. doi:http://dx.doi.org/10.1177/0954407014556114 [in press].
[3] Chow A, Wyszynski ML. Thermodynamic modelling of complete engine systems – a review. Proc Inst Mech Eng, Part D 1999;213:403–15.
[4] Rakopoulos CD, Giakoumis EG. Review of thermodynamic diesel engine simulations under transient operating conditions. SAE 2006-01-0884; 2006.
[5] Seykens XLJ. Development and validation of a phenomenological diesel engine combustion model/door Xander Lambertus Jacobus Seykens.: Technische Universiteit Eindhoven; 2010.
[6] Uzun Abdullah. A parametric study for specific fuel consumption of an intercooled diesel engine using a neural network. Fuel 2012;93:189–99.
[7] de Lucas A, Carmonaa M, Duran A, Lapuertab M. Modeling diesel particulate emissions with neural networks. Fuel 2001;80:539–48.
[8] Kao Minghui, Moskwa John J. Turbocharged diesel engine modeling for nonlinear engine control and state estimation. ASME J Dyn Syst, Meas Control 1995;117(3).
[9] Jensen JP, Kristensen AF, Sorenson SC, Houbak N, Hendricks E. Mean value modeling of a small turbocharged diesel engine. SAE technical paper 910070; 1991.
[10] Zito G, Landau ID. Narmax model identification of a variable geometry turbocharged diesel engine. In: American control conference, vol. 2; 2005. p. 1021–6.
[11] Nikzadfar K, Shamekhi AH. Developing a state space model for a turbocharged diesel engine using the subspace identification method. Proc IMechE Part D: J Automob Eng 2011;225:1692–706.
[12] Zhang Jian, Lan Hehui. Fuzzy modeling of diesel engine based on working position. In: International conference on system science and engineering (ICSSE). Dalian, Liaoning; 2012. p. 514–7.
[13] Qiang Han, Fuyuan Yang, Ming Zhou, Minggao Ouyang. Study on modeling method for common rail diesel engine calibration and optimization. SAE 2004-01-0426; 2004.
[14] SchuK ler M, Nelles O, Isermann R, Hafner M. Fast neural networks for diesel engine control design. Control Eng Pract 2000;8:1211–21.
[15] Ouladsine Mustapha, Bloch Gerard, Dovifaaz Xavier. Neural modelling and control of a diesel engine with pollution constraints. J Intell Robotic Syst 2004;41:157–71.
[16] Benz M, Onder CH, Guzzella L. Engine emission modeling using a mixed physics and regression approach. J Eng Gas Turbines Power 2010;132(4).
[17] Li Ruixue, Huang Ying, Li Gang, Song He. Control-oriented modeling and analysis for turbocharged diesel engine system. In: International conference on measurement, information and control (ICMIC), vol. 2; 2013. p. 855–60.
[18] Casolia P et al. Development and validation of a "Crank-angle" model of an automotive turbocharged engine for HiL applications. Energy Procedia 2014;45:839–48. ATI 2013-68th Conference of the Italian Thermal Machines Engineering Association.
[19] Giakoumis EG, Alafouzos AI. Study of diesel engine performance and emissions during a Transient Cycle applying an engine mapping-based methodology. Appl Energy 2010;87:1358–65.
[20] Kolmanovsky I, Moraal P, van Nieuwstadt M, Stefanopoulou A. Issues in modeling and control of intake flow in variable geometry turbocharged engines. In: Proceedings of 18th IFIP conference on system modelling and optimization. Detroit; 1997.
[21] Guzzella Lino, Onder Christopher H. Introduction to modeling and control of internal combustion engine systems. Springer; 2010.
[22] Ericson Claes, Westerberg Björn, Egnell Rolf. Transient emission predictions with quasi stationary models. SAE Technical Paper 2005-01-3852; 2005.

[23] Pearson Ronald K, Pottmann Martin. Gray-box identification of block-oriented nonlinear models. J Process Control 2000;10(4):301–15.
[24] Gauthier Christophe, Sename Olivier, Dugard Luc, Meissonnier Guillaume. Modeling of a diesel engine common rail injection system. In: IFAC 2005; 2005.
[25] Dinescu DC, Tazerout M. Mean value modeling of a variable nozzle turbocharger (VNT). U.P. Bucharest Scientific Bulletin, Series D, vol. 72(1); 2010. p. 109–16.
[26] Stricker Karla, Kocher Lyle, Koeberlein E, Van Alstine DG, Shaver Gregory M. Turbocharger map reduction for control-oriented modeling. ASME J Dyn Syst, Meas Control 2014;136(4).
[27] Hendricks E, Chevalier A, Jensen M, Sorenson S. Modelling of the intake manifold filling dynamics. SAE technical paper 960037; 1996.
[28] Upadhyay D, Utkin VI, Rizzoni G. Multivariable control design for intake flow regulation of diesel engine using sliding mode. In: 15th Triennial world congress, Barcelona, Spain, 21–26 July; 2002.
[29] Nikzadfar Kamyar, Shamekhi Amir H. Investigating the relative contribution of operational parameters on performance and emissions of a common-rail diesel engine using neural network. Fuel 2014;125:116–28.
[30] Niederreiter Harald. Low-discrepancy and low-dispersion sequences. J Number Theory 1988;30:51–70.
[31] Bishop, Christopher M. Bayesian methods for neural networks. In: Oxford lectures on neural networks. Oxford University Press; 1995.
[32] Lampinen Jouko, Vehtari Aki. Bayesian approach for neural networks – review and case studies. Neural Netw 2001;14(3):7–24.